Analyst

ROYAL SOCIETY OF CHEMISTRY

PAPER

View Article Online
View Journal | View Issue

Cite this: *Analyst*, 2022, **147**, 897

The laccase mediator system at carbon nanotubes for anthracene oxidation and femtomolar electrochemical biosensing†

Ilaria Sorrentino, [a] Marie Carrière,[a] Hélène Jamet,[a] Ilaria Stanzione, [b] Alessandra Piscitelli, [b] Paola Giardina *[b] and Alan Le Goff *[a]

We investigated the use of POXA1b laccase from *Pleurotus ostreatus* for the oxidation of anthracene into anthraquinone. We show that different pathways can occur depending on the nature of the redox mediator combined to laccase, leading to different structural isomers. The laccase combined with 2,2′-azine-bis(3-ethylbenzothiazoline-6-sulfonic acid (ABTS) leads to the formation of 1,4-anthraquinone and/or 1,2-anthraquinone. The unprecedented role of carbon nanotubes (CNTs) as redox mediators for oxidation of anthracene into 9,10-anthraquinone is shown and corroborated by density-functional theory (DFT) calculations. Owing to the efficient adsorption of anthraquinones at CNT electrodes, anthracene can be detected with low limit-of-detection using either laccase in solution, CNT-supported laccase or laccase immobilized at magnetic beads exploiting the adhesive property of a chimeric hydrophobin-laccase.

Received 18th November 2021,
Accepted 2nd February 2022

DOI: 10.1039/d1an02091a

rsc.li/analyst

Introduction

Polycyclic aromatic hydrocarbons (PAHs), aromatic molecules consisting of at least two fused benzenic rings, are well-known environmental and food pollutants. Accumulating PAHs have detrimental effects on flora and fauna and are an increasing health problem as human carcinogens. PAHs can be either produced by food processing (baking, smoking, roasting) or introduced by contamination. PAHs can also be a marker of important environmental pollution of water by oil. Current methods for PAH sensing are based on gas or liquid chromatography coupled to mass spectrometry, fluorimetry or UV-visible spectroscopy.[1] In order to avoid these heavy laboratory instrumentation and/or expensive light sources, electrochemical sensors have represented an easy-to-use and inexpensive alternative. However, PAHs are difficult to detect by electrochemical methods. Most PAHs have high and irreversible oxidation potential. This is the reason why most electrochemical sensors rely on high-potential detection or rely on the detection of oxidized hydroxylated PAHs.[1]

Enzyme-based electrochemical biosensors have relied on both the specificity of enzyme towards specific substrates and the catalytic activity of enzyme to provide high sensitive responses.[2,3] Furthermore, enzyme-based biosensors also rely on the ability of enzymes to perform specific reactions in water at room temperature and atmospheric pressure. During the last decade, the combination of enzymes with nanomaterials have led to tremendous progress in biosensor design and sensitivity.[3–5] In particular, carbon nanotubes (CNTs) have represented a multifunctional material, combining high affinity and biocompatibility towards enzymes, improved electron transfer rates and conductivity and high electroactive surfaces.[2–4,6] Magnetic beads have also represented a versatile material with many advantages in biosensing.[7,8] Apart from their ability to be modified with many types of biomolecules, the use of magnetic beads allows the catalyst or the analyte to be separated or concentrated from the medium.[7,8] Furthermore, magnetic particles can also carry analytes or transducers in microfluidic chips for multiplex analysis.[9,10]

Laccases (*p*-diphenol-dioxygenoxidoreductases; EC 1.10.3.2) are copper-containing oxidases, catalyzing the oxidation of a wide range of aromatic substrates while concomitantly reducing O_2 into water. These metalloenzymes are used or envisioned in industrial applications such as remediation, bleaching, biosensing and fuel cells.[11–13] The active site of laccase is composed of a type 2/type 3 trinuclear copper cluster where O_2 is reduced into water. Electrons are transferred from a mononuclear type 1 copper centre, near the surface of the protein, where the substrate is oxidized. POXA1b, a laccase from *Pleurotus ostreatus*, possess interesting properties for many applications: high stability, high enzymatic activity over a wide

[a]*Univ. Grenoble Alpes, CNRS, DCM, 38000 Grenoble, France. E-mail: alan.le-goff@univ-grenoble-alpes.fr*
[b]*Department of Chemical Sciences, University of Naples Federico II, 80126 Naples, Italy. E-mail: giardina@unina.it*

†Electronic supplementary information (ESI) available: Experimental details, Fig. S1. See DOI: 10.1039/d1an02091a

range of pHs and temperatures and a high redox potential.[14,15] We recently investigated this particular laccase at modified graphene and CNT-based electrodes.[12] For biosensing applications, laccases have been mostly studied for the detection of *ortho*-diphenol substrates such as catechol or dopamine.[16–19] We recently produced in *Pichia pastoris* a chimera by fusion of POXA1b with a hydrophobin, a self-assembling adhesive protein produced by the same fungus *P. ostreatus*, making laccase prone to be immobilized at different types of materials such polystyrene beads, graphene nanosheets or CNTs.[16,18,20]

Laccase redox mediators, the most common being the diammonium salt of 2,2′-azine-bis(3-ethylbenzothiazoline-6-sulfonic acid (ABTS), have been used for many years, acting as electron relays when laccase are immobilized at electrode surface[12,13] or acting as an enhancer/promoter of the ability of laccase to catalyze the oxidation of high potential nonphenolic substrate.[21] Several studies have shown that this so-called laccase-mediator system is able to oxidize several PAHs such as anthracene or benzo(a)pyrene into quinoid products.[22–24] In this work, we intend to design the first example of a PAH electrochemical enzyme sensor by exploring the oxidation of PAHs by laccase and the detection of the quinoid products at multi-walled CNT (MWCNT) electrodes. Porous carbon materials are notorious adsorbents of PAHs, owing to the strong pi–pi-stacking of pi-extended aromatic with CNT sidewalls of CNTs or graphene-based materials.[25–32] We therefore investigate the oxidation of PAH by laccase and the subsequent adsorption and detection of their corresponding enzymatically-oxidized products at MWCNT electrodes. We also investigated the role of CNTs as redox mediator of anthracene oxidation. The versatility of this biosensing strategy was finally studied by using laccase either in solution or immobilized at both CNT and magnetic beads.

Results and discussion

Electrochemical study of the adsorption of anthraquinone on MWCNT electrodes

In order to develop a biosensor based on the detection of oxidation products of anthracene, the detection of adsorbed anthraquinone at MWCNTs was investigated. Among the products of anthracene oxidation, either by chemical or biochemical processes, the main redox-active products of anthracene oxidation are either 1,4-anthraquinone, 1,2-anthraquinone and 9,10-anthraquinone,[33,34] while co-products or products of further oxidation are non-electroactive. In particular, major products of anthracene oxidation by the white rot fungus *P. ostreatus* have been identified as 9,10-anthraquinone and anthracene *trans*-1,2-dihydrodiol.[34] First, the ability of MWCNT electrodes to detect anthraquinone derivatives were tested on two anthraquinone isomers, 1,4-anthraquinone and 9,10-anthraquinone. MWCNTs are well-known to strongly interact with polycyclic aromatics *via* pi–pi interactions with CNT sidewalls. Fig. 1 shows the electrochemical response of MWCNT electrodes previously incubated in a 1 mM solution of

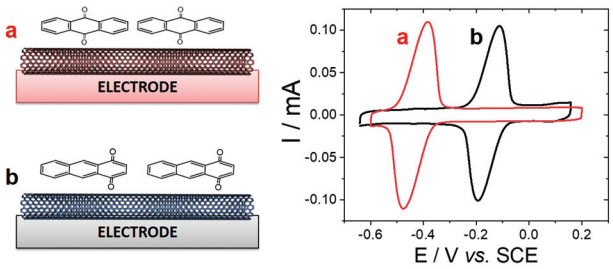

Fig. 1 Schematic representation of adsorbed (a) 9,10-anthraquinone and 1,4-anthraquinone at MWCNT electrode and CV of the modified MWCNT electrodes performed in 0.1 M McIlvaine buffer pH 5 (v = 10 mV s^{-1}, pH 7) after incubation (10 min, 25 °C) of the MWCNT electrode in a 1 mM MeCN solution of (a) 9,10-anthaquinone and (b) 1,4-anthraquinone.

1,4-anthraquinone or 9,10-anthraquinone in MeCN. In order to avoid any interferences from redox-active impurities, high-purity (99%) MWCNTs were chosen. No background electroactivity of the MWCNT electrode was observed in the experimental potential window.

The electrodes were further washed and the adsorption of respective anthraquinones was studied in 0.1 M phosphate buffer. The expected redox reversible systems observed at $E_{p,1/2}$ = −0.43 V (ΔE = 90 mV) and $E_{p,1/2}$ = −0.12 V *vs.* SCE correspond to the redox potential of 9,10-anthraquinone and 1,4-anthraquinone respectively. Both systems correspond to the two-electron/two-proton oxidation of anthraquinone into their corresponding bis-paraphenol product.[35–37] According to integration of the charge, similar maximum surface concentrations of 0.82 and 0.71 nmol cm^{-2} were measured for 1,4-anthraquinone and 9,10-anthraquinone respectively.

With the aim of further describing the adsorption of anthraquinone at MWCNTs, an equilibrium isotherm model was investigated using different concentrations of anthraquinone (Fig. 2).

The adsorption isotherm was studied by investigating the anthraquinone redox system by square-wave voltammetry

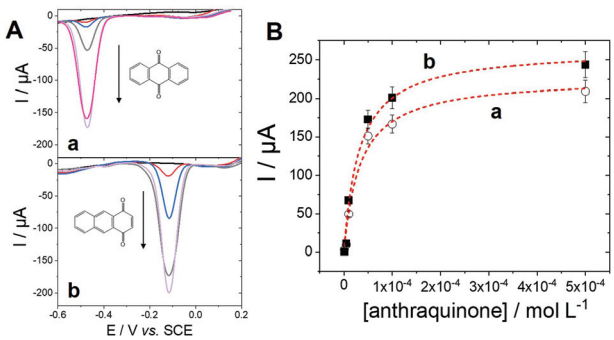

Fig. 2 (A) SWV and (B) corresponding plot of the peak current against anthraquinone concentration (0.1 M McIlvaine buffer pH 5, 25 °C, pulse height = 25 mV, pulse width = 0.5 s, step height = −5 mV) performed after incubation (10 min, 25 °C) of the MWCNT electrode in a MeCN solution of (a, ○) 9,10-anthaquinone and (b, ■) 1,4-anthraquinone at different concentrations.

(SWV) obtained after incubation at different anthraquinone concentrations. SWV is employed as it provides high sensitivity towards the detection of such reversible redox signals, reducing signal-to-noise ratio and background capacitive currents. As expected, the intensity of the peak for each anthraquinone increases when increasing the incubating concentration until reaching a plateau. This behaviour was well modelized by using a simple Langmuir isotherm model according to eqn (1):[38–40]

$$I_{p,eq} = \frac{I_{p,max} \times K_{AQ} \times [AQ]}{1 + K_{AQ} \times [AQ]} \quad (1)$$

where $I_{p,eq}$ is the equilibrium peak current, $I_{p,max}$ is the peak current at saturating concentrations of 1.4-anthraquinone or 9,10-anthraquinone and K_{AQ} is the association constant between AQ and MWCNT surface in MeCN at 25 °C. For 1,4-anthraquinone, the best fit (R^2 = 0.98) was achieved with a $I_{p,max}$ = 260(±16) μA and $K_{1,4\text{-}AQ}$ = 3.2(±0.7) × 10^5 L mol^{-1}. For 9,10-anthraquinone, the best fit (R^2 = 0.98) was achieved with a $I_{p,max}$ = 230(±15) μA and $K_{9,10\text{-}AQ}$ = 3.0(±0.7) × 10^5 L mol^{-1}. For comparison, an association constant 1 to 2 × 10^3 L mol^{-1} have been measured for pyrene and different types of pyrene-based derivatives.[27,40,41] As expected, both anthraquinone derivatives exhibit the same interaction mechanism with MWCNT sidewalls. These results underline that MWCNT electrodes are able to reproducibly adsorb and detect anthraquinone isomers *via* a Langmuir-type reversible model.

Electrochemical detection of the products of anthracene oxidation by free and adsorbed laccase with and without ABTS

Using the ability of MWCNT electrodes to detect anthraquinone derivatives, we investigate the detection of the products of the enzymatic oxidation of anthracene by laccase, either in solution or adsorbed at the surface of the MWCNT electrodes. In most cases, the use of a redox mediator such as ABTS is required for laccases to be able to oxidize nonphenolic compounds such as PAHs.[21] POXA1b laccase was chosen for its high redox potential, high activity and stability and its thermophilic character[42] suitable for the oxidation of nonphenolic compounds. We have recently shown its facile adsorption on MWCNT electrodes for sensitive catechol and dopamine sensing.[20] Fig. 3 shows the detection of anthraquinone products at different concentrations of anthracene in the presence of POXA1b laccase in solution or adsorbed at MWCNT electrodes, with and without ABTS. When laccase is used in solution, no anthraquinone derivatives were detected at room temperature after incubation of laccase (1 U mL^{-1}) and 100 μM of anthracene. When temperature is increased to 40 °C, traces of 9,10-anthraquinone are detected at MWCNT electrodes with maximum SWV peak current of 5.5 μA (E_p = −0.42 V) at 100 μM of anthracene (Fig. 3A). When the incubation is performed in the presence of ABTS (20 mM), a SWV peak is observed at E_p = −0.06 V, likely corresponding to the production of 1,2- or/and 1,4-anthraquinone (Fig. 3B). This product is detected at extremely low limit-of-detection of 0.1 fM and the signal levels off at current values of 122 μA at 100 μM of anthracene. At this concentration, a small peak is also observed at E_p = −0.42 V, corresponding to the concomitant formation of 9,10-anthraquinone, only observed at high anthracene concentrations.

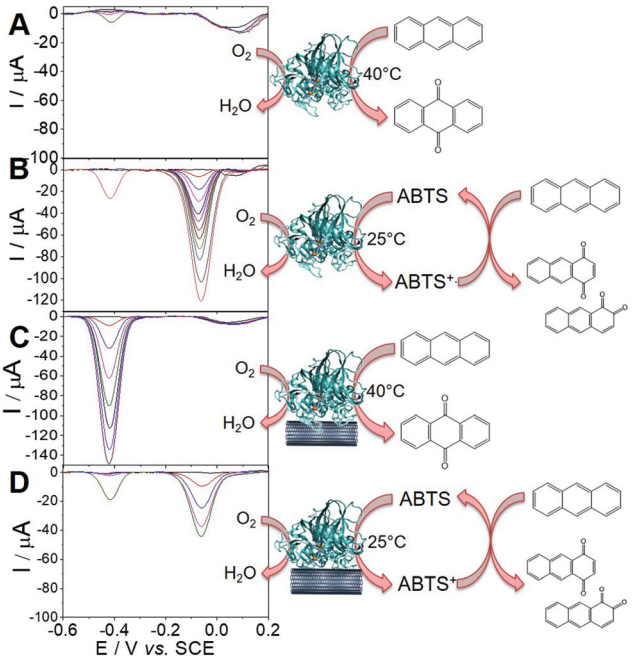

Fig. 3 (A) SWV (0.1 M McIlvaine buffer pH 5, 25 °C, pulse height = 25 mV, pulse width = 0.5 s, step height = −5 mV) for the detection of different concentrations of anthracene (0, 0.1 nM, 100 nM, 1 μM and 100 μM) after incubation (10 min) of the MWCNT electrode in a solution of 1 U mL^{-1} of laccase and anthracene left to react for 2 h at 40 °C min; (B) SWV for the detection of different concentrations of anthracene (0, 0.1 fM, 0.5 fM, 1 fM, 10 fM, 50 fM, 0.1 pM, 1 pM, 10 pM, 0.05 nM, 1 μM and 100 μM) after incubation (10 min) of the MWCNT electrode in a solution of 1 U mL^{-1} of laccase and ABTS left to react for 1 h at 25 °C min; (C) SWV for the detection of different concentrations of anthracene (0, 0.1 nM, 10 nM, 0.1 μM, 1 μM, 10 μM and 100 μM) after incubation (10 min) of a POXA1b modified electrode in a solution of anthracene left to react for 2 h at 40 °C; (D) SWV for the detection of different concentrations of anthracene after incubation (10 min) of a POXA1b-modified electrode in a solution of anthracene (0, 0.1 nM, 100 nM, 1 μM and 100 μM) and ABTS left to react for 1 h at 25 °C.

For MWCNT-supported laccases, without addition of ABTS, 9,10-anthraquinone is detected at concentrations of 0.1 nM, levelling at 100 μM with maximum current of −148 μA (Fig. 3C). When ABTS is used in solution with MWCNT-supported laccase, 1,2- or/and 1,4-anthraquinone is mostly detected with maximum current of 45 μA at E_p = −0.06 V at 100 μM of anthracene, with the concomitant formation of 9,10-anthraquinone at E_p = −0.41 V (Fig. 3D).

These results show that the formation of these anthraquinone isomers can be obtained from the enzymatic oxidation of anthracene by laccases, depending on the conditions and the presence and nature of the redox mediator. When ABTS is used either with laccase in solution or adsorbed on MWCNTs, 1,2- and or 1,4-anthraquinone are the major products of the

oxidation of anthracene. The fact that negligible amounts of anthraquinone is observed when laccase is used in solution without ABTS is expected from the fact that laccases are known to have poor oxidation ability of nonphenolic substrates without the addition of a redox mediator. However, owing to the stability of POXA1b at temperature up to 40 °C, traces of 9,10-anthraquinone can still be observed. More interestingly, despite the fact that adsorbed laccase is present in low amounts as compared to laccase in solution (2 U), the formation of 9,10-anthraquinone is detected when laccases is adsorbed at MWCNT electrodes, without the need of a redox mediator in solution.

To further investigate the role of MWCNTs in the oxidation of anthracene by laccases in the absence of ABTS, DFT calculations were done. The idea was to compare the electronic structure of the anthracene adsorbed at MWCNT electrodes or in solution. To modelize the anthracene adsorbed at MWCNT electrodes, we used a graphene ribbon of 18 × 12 Å^2. Fig. 4 reports the highest occupied orbitals HOMO, HOMO−1 of the two systems. The orbitals involved in the oxidation of the anthracene are the HOMO for the molecule isolated and the HOMO−1 for the anthracene adsorbed on the graphene. These two orbitals are localized similarly on carbon atoms of anthracene but the energy of the orbital involved for the model of the anthracene adsorbed is higher in energy (−6.93 eV against −7.29 eV). Therefore, DFT calculations underline the fact that anthracene is easier to oxidize when adsorbed at the surface of MWCNTs. This explains the difference of reactivity observed experimentally and that laccases do not need redox mediators such as ABTS when anthracene is adsorbed on MWCNTs, the latter acting as oxidation promoters.

SWV experiments performed in the best conditions, *i.e.* adsorbed laccases without ABTS and laccase in solution with ABTS, were modelized using adsorption isotherms considering the fact that a pseudo-equilibrium is reached during the oxidation of anthracene (Fig. 5A). No accurate model was obtained using a simple Langmuir isotherm, likely arising from the presence of a mixture of enzymes, anthracene and anthraquinone at MWCNT electrodes. In this particular case

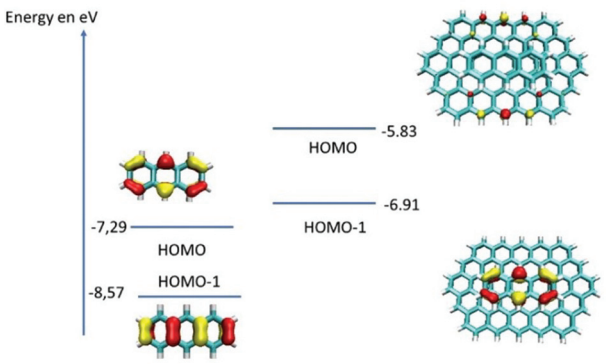

Fig. 4 Schematic representation of the highest occupied orbitals for the anthracene and for the model of the anthracene adsorbed at MWCNT electrodes.

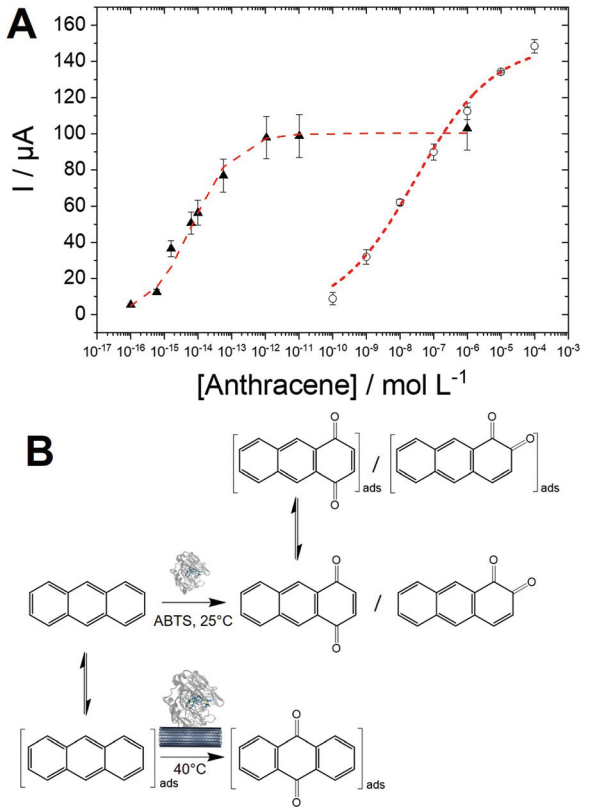

Fig. 5 (A) Logarithmic plot of the SWV peak current towards anthracene concentration for the detection of anthracene at MWWCNT electrode from (▲) a solution of 1 U mL^{-1} of laccase and ABTS left to react for 1 h at 25 °C min and (○) from a POXA1b-modified MWCNT electrode in a solution of anthracene left to react for 2 h at 40 °C; (B) hypothesized mechanism for the formation of 1,4-anthraquinone and 9,10-anthraquinone and their adsorption on MWCNT.

where heterogeneity of adsorptions might be caused by a complicated mixture at such porous surface, the Freundlich model was successfully used to fit the experimental data, according to eqn (2):[38,43]

$$I_{p,eq} = \frac{I_{p,max} \times (K_{AQ}^{app} \times [anthracene])^n}{1 + (K_{AQ}^{app} \times [anthracene])^n} \quad (2)$$

where $I_{p,eq}$ is the equilibrium peak current, $I_{p,max}$ is the peak current at saturating concentrations of anthracene and K_{AQ} is the association constant between the as-produced anthraquinone (AQ) derivative and the MWCNT surface in water and n is Langmuir–Freundlich coefficient number. Table 1 shows the

Table 1 Fitting parameters for the Langmuir–Freundlich isotherm model from Fig. 5A

	$I_{p,max}$	K_{AQ}^{app} (L mol^{-1})	n	R^2
Laccase/ABTS	100(±9)	1.5×10^{14}	0.7(±0.1)	0.975
Laccase/MWCNT	150(±7)	3.5×10^{7}	0.4(±0.1)	0.997

Langmuir–Freundlich model parameters obtained from fitting curves of Fig. 5A.

The high apparent value of K_{AQ} of 1.5×10^{14} L mol^{-1} for the laccase/ABTS mediator system is likely due to the high efficiency of the enzymatic oxidation, which maximizes the formation of 1,4-anthraquinone and its subsequent adsorption on MWCNT surfaces. The K_{AQ}^{app} value is also several order of magnitude higher compared to the K_{AQ} value measured for anthraquinone adsorption in MeCN. This is expected from the stronger pi–pi interaction between anthraquinone and CNT sidewalls in water as compared to MeCN. K_{AQ}^{app} value of 3.5×10^7 L mol^{-1} for MWCNT-supported laccase, is indicative of a less-efficient oxidation process as compared to the laccase/ABTS mediator system, generating lower amounts of 9,10-anthraquinone. The fact that higher I_p^{max} of 150 μA is obtained for the MWCNT-supported laccase system likely arises from two reasons.

The oxidation process, in this case, is driven by the adsorption of anthracene which might have higher amounts of binding site on MWCNT sidewalls as compared to anthraquinone. ABTS can also possibly compete with anthraquinone towards binding sites in the case of the laccase/ABTS system. These results indicate that two major pathways are involved in the anthracene oxidation by laccases (Fig. 5B). First, the most sensitive and efficient way is the use of the laccase/ABTS system in solution. This allows the fast generation of 1,4-anthraquinone, which is subsequently adsorbed on MWCNTs and detected by SWV at detection limits as low as 0.1 fM. A second pathway is observed in the case of MWCNT-supported laccase, producing specifically 9,10-anthraquinone. The fact that this reaction is only observed when laccase is immobilized on MWCNT implies that MWCNT plays the role of the redox mediator by oxidizing adsorbed anthracene. Electrons are likely transferred from MWCNTs to the laccase active site, affording the oxidation of anthracene into 9,10-anthraquinone. We recently demonstrated that POXA1b could favourably transfer electrons between the T1 active site and the electrode for direct oxygen reduction.[20] This pathway leads to the preferred formation of 9,10-anthraquinone over 1,4- and 1,2-anthraquinone. The selectivity of the oxidation of anthracene *via* these two pathways is still not clearly understood. However, we can hypothesize that a radical intermediate formed by anthracene oxidation is likely stabilized by pi–pi interactions with MWCNTs. It is noteworthy that the high-potential electro-oxidation of anthracene at CNT-based electrodes leads to the formation of 9,10-anthaquinone.[44]

Anthracene and PAH biosensing performances

Owing to the logarithmic scale, a linear range for the biosensing of anthracene could be obtained for the laccase/ABTS and the laccase/MWCNT systems. Furthermore, we also took advantage of the engineered laccase-hydrophobin chimera to modify commercial magnetic beads. This strategy was employed to underline the versatility of this type of PAH biosensors and to demonstrate the possibility to integrate this sensing strategy in future magnetic-bead-based biosensing platform. The immobilization procedure was easy and fast, since no derivatization procedure was necessary, and allowed to obtain 70% immobilization yield. The immobilized laccase showed high stability, retaining almost total activity after 28 days of storage at both 4° and 25 °C. These biofunctionalized magnetic beads were also used with ABTS to provide anthracene biosensing in solution. Fig. 6 displays the linear region for all three configurations towards anthracene concentrations. The performances of the three configurations are given in Table 2.

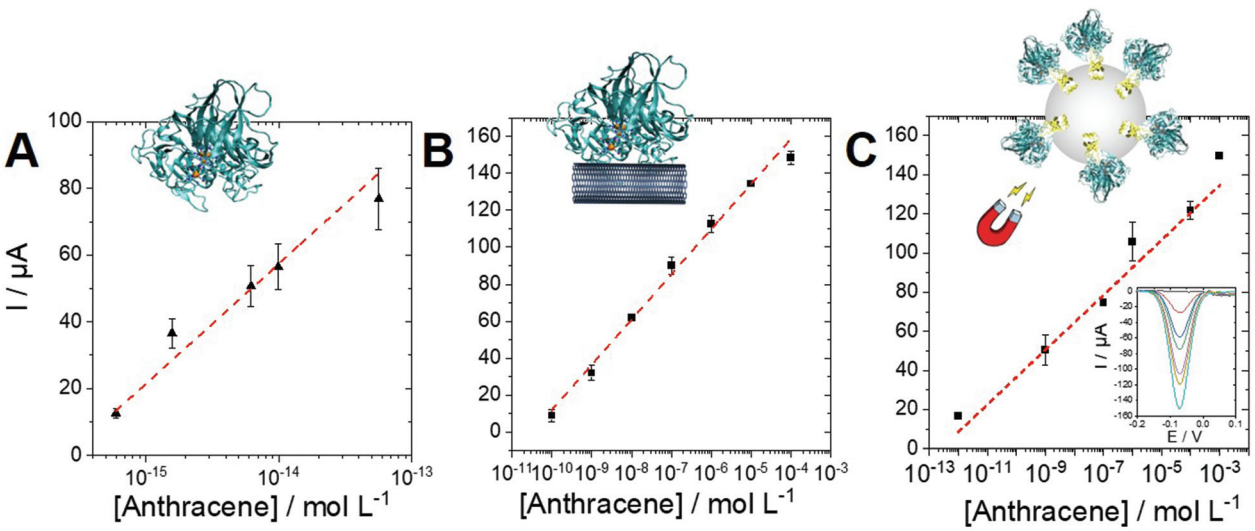

Fig. 6 Linear part of the logarithmic plot of the SWV peak current against anthracene concentration for the detection of anthracene at MWCNT electrode from (A) a solution of 1 U mL^{-1} of laccase and 20 mM ABTS left to react for 1 h at 25 °C min, (B) from a POXA1b-modified MWCNT electrode in a solution of anthracene left to react for 2 h at 40 °C and (C) a solution of 20 mU mL^{-1} of biofunctionaized microbeads and 50 mM ABTS left to react for 1 h at 25 °C min (inset: corresponding SWV performed in a 0.1 M phosphate/citrate buffer solution pH 5).

Table 2 Electrochemical parameters for anthracene biosensing

	Sensitivity	Linear range	R^2
Laccase/ABTS	36(±4)	0.6 fM–0.1 pM	0.966
Laccase/MWCNT	24.4(±0.6)	0.1 nM–0.1 mM	0.997
MB-laccase/ABTS	14(±2)	1 pM–1 mM	0.960

As expected, the best sensitivity and LOD (0.6 fM) is obtained for the laccase/ABTS system in solution with excellent repeatability (performed on three electrodes). This originates for the high concentration of enzyme (1 U mL^{-1}) and the efficiency of the laccase/ABTS system towards anthracene oxidation. The laccase/MWCNT system (without the use of ABTS) exhibits a higher LOD of 0.1 nM but a wider linear range between 0.1 nM and 0.1 mM. The chimera-modified magnetic beads exhibit a lower sensitivity of 14 μA per log unit as compared to the laccase/ABTS system. This is caused by the lower activity of the biofunctionalized beads (10 mU L^{-1}), as compared to laccase in solution (1 U mL^{-1}). However, this lower activity affords a lower production of 1,4-anthraquinone and a higher linear range between 1 pM and 1 mM. These results underline the fact that a wide linear range and an extremely low LOD can be obtained depending on the biosensing conditions. These conditions can be easily adapted depending on the concentration range of the starting anthracene solution.

Owing to the high sensitivity of the laccase mediator system based on laccase and ABTS in solution and the ability of MWCNT electrodes to sensibly detect anthraquinone, the biosensing of different PAHs were studied using this strategy. Fig. S1† shows the oxidation of pyrene and benzo(a)pyrene, two well-known PAHs. By performing a logarithmic fit, calibration curves were obtained for all PAHs. Table 3 summarizes the analytical performances of the biosensors.

It is noteworthy that a one—order-of-magnitude difference is observed compared to anthracene biosensing, arising from the lower efficiency of the oxidation process for both pyrene and benzo(a)pyrene by the laccase/ABTS system.

This is the first example of a PAH biosensor based on an enzymatic process. For comparison, few electrochemical biosensors for PAH have been developed, only based on affinity-type receptors such as antibody/antigen interaction. A biosensor based on the interaction of PAH with DNA was able to detect PAH by DPV at high potential (1 V) with a LOD of 10 nM.[45] Other type of electrochemical sensor are mostly based on the high potential oxidation of PAH on different electrode materials.[1] Polyaniline-based nanostructured electrodes exhibit LOD of 4.4 nM and 0.1 fM for anthracene and phenanthrene respectively[46–48] Direct electrochemical detection of monohydroxylated PAHs by conjugated polyelectrolyte/graphene-based electrodes exhibits LOD of 1.4 nM.[49] Imprinted polymers have also been used, showing LOD of 0.5 fM and sensitivity of 80 μA per log unit.[50] Cadmium/aluminum layered double hydroxide-based electrodes[51] are able to interact with anthracene and its electrochemical sensing was achieved at −0.92 V in 1 M KOH by DPV with a sensitivity of 1.9 μA per log unit, a linear range of 0.1 to 100 pM and a LOD of 0.5 fM.

Table 3 Electrochemical parameters for pyrene and benzo(a)pyrene biosensing

	Sensitivity	Linear range	R^2
Pyrene	3.6(±0.1)	1 fM–10 pM	0.998
Benzo(a)pyrene	3.5(±0.4)	1 fM–10 pM	0.979

Conclusions

In this work we developed a novel strategy for oxidation and detection of PAH using a combination of laccase and MWCNT electrodes. Owing to the high sensitivity of MWCNT electrodes towards quinones, the products of the oxidation of PAHs can be adsorbed and detected at MWCNT electrodes using SWV. The study of anthracene oxidation by the thermophilic POXA1b shows that MWCNTs can play the role of a redox mediator towards oxidation of anthracene into 9,10-anthraquinone, as confirmed by SWV experiments and DFT calculations. Using ABTS, 1,4- and/or 1,2-anthraquinone are preferably formed and provide the most efficient way of anthracene oxidation and detection. A highly sensitive biosensor of anthracene was designed with extremely low LOD of 0.6 fM and a linear range which can be easily adapted depending on the biosensing conditions. Owing to the flexibility of laccase and its hydrophobin chimera, laccase-modified magnetic beads can also be employed in combination with MWCNT electrodes for anthracene detection. Furthermore, this biosensor can be extended to other PAH such as pyrene or benzo(a)-pyrene. This study paves the way for the use of laccase and laccase-modified nanomaterials for the design of highly efficient PAH oxidation and detection systems.

Author contributions

Project administration, funding acquisition, conceptualization: P. G. and A. L. G. writing, review and editing: A. P., H. J., P. G. and A. L. G., investigation, methodology, formal analysis: I. S., M. C., H. J. and A. P.

Conflicts of interest

There are no conflicts to declare.

Acknowledgements

This project is funded by Italian Education, University and Research Ministry (MIUR), French National Research Agency (ANR) and co-funded by European Union's Horizon 2020 research and innovation program under the framework of ERA-NET Cofund MarTERA (Maritime and Marine

Technologies for a new Era). This work was supported by the Agence Nationale de la Recherche through the LabEx ARCANE programe (ANR-11-LABX-0003-01) and the Graduate School on Chemistry, Biology and Health of Univ Grenoble Alpes CBH-EUR-GS (ANR-17-EURE-0003). The authors acknowledge support from the plateforme de Chimie NanoBio ICMG FR 2607 (PCN-ICMG).

Notes and references

1 S. A. Nsibande, H. Montaseri and P. B. C. Forbes, *TrAC, Trends Anal. Chem.*, 2019, **115**, 52–69.
2 A. Le Goff, M. Holzinger and S. Cosnier, *Analyst*, 2011, 1279–1287.
3 M. Holzinger, A. Le Goff and S. Cosnier, *Sensors*, 2017, **17**, 1010.
4 M. Holzinger, A. Le Goff and S. Cosnier, *Front. Chem.*, 2014, **2**, 63.
5 H. Ju, *Appl. Mater. Today*, 2018, **10**, 51–71.
6 A. Le Goff and M. Holzinger, *Sustainable Energy Fuels*, 2018, **2**, 2555–2566.
7 J. B. Haun, T.-J. Yoon, H. Lee and R. Weissleder, *WIREs Nanomed. Nanobiotechnol.*, 2010, **2**, 291–304.
8 X. He, H. Huo, K. Wang, W. Tan, P. Gong and J. Ge, *Talanta*, 2007, **73**, 764–769.
9 C. Sun, J. S. H. Lee and M. Zhang, *Adv. Drug Delivery Rev.*, 2008, **60**, 1252–1265.
10 T. Konry, S. S. Bale, A. Bhushan, K. Shen, E. Seker, B. Polyak and M. Yarmush, *Microchim. Acta*, 2012, **176**, 251–269.
11 C. Pezzella, L. Guarino and A. Piscitelli, *Cell. Mol. Life Sci.*, 2015, **72**, 923–940.
12 A. Le Goff, M. Holzinger and S. Cosnier, *Cell. Mol. Life Sci.*, 2015, **72**, 941–952.
13 N. Mano and A. de Poulpiquet, *Chem. Rev.*, 2017, **118**, 2392–2468.
14 C. Pezzella, V. G. Giacobelli, V. Lettera, G. Olivieri, P. Cicatiello, G. Sannia and A. Piscitelli, *J. Biotechnol.*, 2017, **259**, 175–181.
15 A. M. Garzillo, M. C. Colao, V. Buonocore, R. Oliva, L. Falcigno, M. Saviano, A. M. Santoro, R. Zappala, R. P. Bonomo, C. Bianco, P. Giardina, G. Palmieri and G. Sannia, *J. Protein Chem.*, 2001, **20**, 191–201.
16 I. Sorrentino, I. Stanzione, Y. Nedellec, A. Piscitelli, P. Giardina and A. Le Goff, *Int. J. Mol. Sci.*, 2020, **21**, 3741.
17 M. M. Rodríguez-Delgado, G. S. Alemán-Nava, J. M. Rodríguez-Delgado, G. Dieck-Assad, S. O. Martínez-Chapa, D. Barceló and R. Parra, *TrAC, Trends Anal. Chem.*, 2015, **74**, 21–45.
18 I. Sorrentino, P. Giardina and A. Piscitelli, *Appl. Microbiol. Biotechnol.*, 2019, **103**, 3061–3071.
19 S. Palanisamy, S. K. Ramaraj, S.-M. Chen, T. C. K. Yang, P. Yi-Fan, T.-W. Chen, V. Velusamy and S. Selvam, *Sci. Rep.*, 2017, **7**, 1–12.
20 I. Sorrentino, I. Stanzione, A. Piscitelli, P. Giardina and A. Le Goff, *Biosens. Bioelectron.: X*, 2021, 100074.
21 O. V. Morozova, G. P. Shumakovich, S. V. Shleev and Ya. I. Yaropolov, *Appl. Biochem. Microbiol.*, 2007, **43**, 523–535.
22 D. E. Dodor, H.-M. Hwang and S. I. N. Ekunwe, *Enzyme Microb. Technol.*, 2004, **35**, 210–217.
23 C. Johannes, A. Majcherczyk and A. Hüttermann, *Appl. Microbiol. Biotechnol.*, 1996, **46**, 313–317.
24 N. N. Pozdnyakova, J. Rodakiewicz-Nowak, O. V. Turkovskaya and J. Haber, *Enzyme Microb. Technol.*, 2006, **39**, 1242–1249.
25 T. G. Hedderman, S. M. Keogh, G. Chambers and H. J. Byrne, *J. Phys. Chem. B*, 2006, **110**, 3895–3901.
26 S. Gotovac, H. Honda, Y. Hattori, K. Takahashi, H. Kanoh and K. Kaneko, *Nano Lett.*, 2007, **7**, 583–587.
27 Y. Kusumoto, *Chem. Phys. Lett.*, 1987, **136**, 535–538.
28 A. Le Goff, K. Gorgy, M. Holzinger, R. Haddad, M. Zimmerman and S. Cosnier, *Chem. – Eur. J.*, 2011, **17**, 10216–10221.
29 B. Reuillard, A. Le Goff, M. Holzinger and S. Cosnier, *J. Mater. Chem. B*, 2014, **2**, 2228–2232.
30 N. Lalaoui, B. Reuillard, C. Philouze, M. Holzinger, S. Cosnier and A. Le Goff, *Organometallics*, 2016, **35**, 2987–2992.
31 A. Le Goff, B. Reuillard and S. Cosnier, *Langmuir*, 2013, **29**, 8736–8742.
32 J. A. Mann, J. Rodríguez-López, H. D. Abruña and W. R. Dichtel, *J. Am. Chem. Soc.*, 2011, **133**, 17614–17617.
33 A. Bruckner and M. Baerns, *Appl. Catal., A*, 1997, **157**, 311–334.
34 L. Bezalel, Y. Hadar, P. P. Fu, J. P. Freeman and C. E. Cerniglia, *Appl. Environ. Microbiol.*, 1996, **62**, 2554–2559.
35 M. Sosna, J.-M. Chrétien, J. D. Kilburn and P. N. Bartlett, *Phys. Chem. Chem. Phys.*, 2010, **12**, 10018–10026.
36 N. Lalaoui, A. Le Goff, M. Holzinger, M. Mermoux and S. Cosnier, *Chem. – Eur. J.*, 2015, **21**, 3198–3201.
37 S. Gentil, S. M. Che Mansor, H. Jamet, S. Cosnier, C. Cavazza and A. Le Goff, *ACS Catal.*, 2018, 3957–3964.
38 S. Sharma and G. P. Agarwal, *Anal. Biochem.*, 2001, **288**, 126–140.
39 R. Puopolo, I. Sorrentino, G. Gallo, A. Piscitelli, P. Giardina, A. Le Goff and G. Fiorentino, *Sci. Rep.*, 2021, **11**, 2991.
40 B. Reuillard, A. Le Goff and S. Cosnier, *Chem. Commun.*, 2014, **50**, 11731–11734.
41 K. Yang, X. Wang, L. Zhu and B. Xing, *Environ. Sci. Technol.*, 2006, **40**, 5804–5810.
42 C. Pezzella, S. Giacobbe, V. G. Giacobelli, L. Guarino, S. Kylic, M. Sener, G. Sannia and A. Piscitelli, *J. Mol. Catal. B: Enzym.*, 2016, **134**, 274–279.
43 F. Haddache, A. Le Goff, B. Reuillard, K. Gorgy, C. Gondran, N. Spinelli, E. Defrancq and S. Cosnier, *Chem. – Eur. J.*, 2014, **20**, 15555–15560.

44 P. Barathi and A. S. Kumar, *Chem. – Eur. J.*, 2013, **19**, 2236–2241.
45 Y. Ni, P. Wang, H. Song, X. Lin and S. Kokot, *Anal. Chim. Acta*, 2014, **821**, 34–40.
46 O. Tovide, N. Jaheed, N. Mohamed, E. Nxusani, C. E. Sunday, A. Tsegaye, R. F. Ajayi, N. Njomo, H. Makelane, M. Bilibana, P. G. Baker, A. Williams, S. Vilakazi, R. Tshikhudo and E. I. Iwuoha, *Electrochim. Acta*, 2014, **128**, 138–148.
47 O. E. Fayemi, A. S. Adekunle and E. E. Ebenso, *J. Nanomater.*, 2016, **2016**, e9614897.
48 O. Tovide, N. Jahed, C. E. Sunday, K. Pokpas, R. F. Ajayi, H. R. Makelane, K. M. Molapo, S. V. John, P. G. Baker and E. I. Iwuoha, *Sens. Actuators, B*, 2014, **205**, 184–192.
49 Y. Pang, Y. Huang, W. Li, L. Feng and X. Shen, *ACS Appl. Nano Mater.*, 2019, **2**, 7785–7794.
50 H. Munawar, J. S. Mankar, M. D. Sharma, A. Garcia-Cruz, L. A. L. Fernandes, M. Peacock and R. J. Krupadam, *Talanta*, 2020, **219**, 121273.
51 X. Qiao, M. Wei, D. Tian, F. Xia, P. Chen and C. Zhou, *J. Electroanal. Chem.*, 2018, **808**, 35–40.